Combination of perturbation theory with the configuration-interaction method

M. G. Kozlov,[1,2] I. I. Tupitsyn,[3] A. I. Bondarev,[4] and D. V. Mironova[2]
[1]*Petersburg Nuclear Physics Institute of NRC "Kurchatov Institute," 188300 Gatchina, Russia*
[2]*St. Petersburg Electrotechnical University "LETI," Prof. Popov Str. 5, 197376 St. Petersburg, Russia*
[3]*Department of Physics, St. Petersburg State University, Ulianovskaya 1, Petrodvorets, 198504 St. Petersburg, Russia*
[4]*Center for Advanced Studies, Peter the Great St. Petersburg Polytechnic University, Polytekhnicheskaja 29, 195251 St. Petersburg Russia*

(Received 4 February 2022; accepted 26 April 2022; published 10 May 2022)

The present atomic theory provides accurate and reliable results for atoms with a small number of valence electrons. However, most current methods of calculations fail when the number of valence electrons exceeds four or five. This means that we cannot make reliable predictions for more than half of the periodic table. Here we suggest a modification of the configuration interaction plus many-body perturbation theory, which may be applicable to atoms and ions with partly filled d and f shells.

DOI: 10.1103/PhysRevA.105.052805

I. INTRODUCTION

At present there are several methods of the relativistic correlation calculations of atoms, such as multiconfiguration Dirac-Fock [1–5], configuration interaction (CI) [6–10], many-body perturbation theory (MBPT) [11–13], CI + MBPT [14–17], coupled cluster [18–22], and others. Calculations are usually done in the no-virtual-pair approximation using Dirac-Coulomb, or Dirac-Coulomb-Breit approximations [23]. QED corrections may be included using radiative potential method [24,25] and QEDMOD potential [26,27].

The coupled cluster method is one of the most popular and effective methods for calculation of atoms with a small number of open-shell electrons (or holes). Calculations of the spectra of atoms and ions with many valence electrons (e.g., transition metals, lanthanides, and actinides) are very difficult and usually not very accurate. The reason for that is a combination of strong correlations and a very large configuration space. To account for strong correlations one needs nonperturbative methods, such as CI. On the other hand, a large configuration space makes such calculations very expensive. As a compromise one can try to combine CI with perturbation theory (PT). We will first assume that all closed atomic shells are considered frozen. Then we are treating only valence correlations and consider a combination of the valence CI with valence perturbation theory (VPT). Later, we will see that this approach can also be used to treat core-valence correlations.

Recently there were several attempts [28–31] to develop an effective and fast CI + VPT method to speed up calculations for such systems, where straightforward CI calculations are impossible. Application of these methods for systems with a large number of valence electrons was demonstrated in Refs. [32,33]. A general idea of all these calculation schemes is to make CI in a smaller subspace P and calculate corrections from a complementary subspace Q using VPT. In Refs. [28–30] it is suggested to neglect nondiagonal blocks of the CI matrix in the subspace Q, which is equivalent to using VPT. All these methods require summation over all many-electron basis states of the complementary subspace Q. Although calculating this sum is much easier than calculating and diagonalizing the whole CI matrix, it is still too expensive for the number of valence electrons approaching, or exceeding ten.

In the paper [30], the sum over determinants was partly substituted by the sum over configurations that led to a significant increase in calculation speed. Here we want to make another step in this direction. To this end, we will partly substitute VPT with many-body perturbation theory (MBPT). The method we propose here is similar to the old CI + MBPT method [14] but uses different splitting of the problem into the CI and MBPT parts. In particular, we suggest to account for double excitations (D) from the subspace P by means of the MBPT and treat single excitations (S) within VPT, or, if possible, include them directly in CI. We think that this variant is not only more efficient for treating valence correlations but may also be used for the core-valence correlations.

II. FORMALISM

A. Valence correlations

Consider a many-electron atom or ion with N valence electrons, where N is of the order of 10. Let us first assume that other electrons always occupy closed core shells, which is known as a frozen-core approximation. Our aim is to solve the N-electron Schrödinger equation and find the spectrum of this system.

We start with splitting N-electron configuration space in two orthogonal subspaces P and Q. The subspace P, which we call valence, includes the most important shells. It may be not obvious from the start, which orbitals are "important." We definitely must include into subspace P all orbitals with occupation numbers of the order of unity in the physical states we are interested in. Complementary subspace Q includes

S, D, and so on excitations from the valence shells to the virtual ones, thus, $Q = Q_S + Q_D + \cdots$. We start by solving the matrix equation in the subspace P,

$$\hat{P}H\hat{P}\Psi_a = E_a\hat{P}\Psi_a, \tag{1}$$

where H is the Hamiltonian for valence electrons and $\hat{P}$ is the projector on the subspace P. We can find a correction from the complementary subspace Q using the second-order perturbation theory:

$$\delta E_a = \sum_{n\in Q} \frac{\langle\Psi_a|\hat{P}H\hat{Q}|n\rangle\langle n|\hat{Q}H\hat{P}|\Psi_a\rangle}{E_a - E_n}, \tag{2}$$

where $|n\rangle$ are N-electron Slater determinants in the complementary subspace Q and $E_n = \langle n|\hat{Q}H\hat{Q}|n\rangle$.

The wave function Ψ_a is a linear combination of the Slater determinants:

$$\Psi_a = \sum_{m\in P} C^a_m|m\rangle = \sum_{p,m_p} C^a_{p,m_p}|p,m_p\rangle. \tag{3}$$

Here and below indexes p and q run over configurations in the subspaces P and Q, respectively, and indexes m_p and n_q numerate determinants within one configuration. Now Eq. (2) takes the form

$$\delta E_a = \sum_{p,m_p}\sum_{p',m_{p'}} C^a_{p,m_p}C^a_{p',m_{p'}}\sum_{q,n_q} \times \frac{\langle p,m_p|H|q,n_q\rangle\langle q,n_q|H|p',m_{p'}\rangle}{E_a - E_{q,n_q}}, \tag{4}$$

where the sum over the subspace Q is also split in two.

For an atom with $N \approx 10$, the dimension of space Q is very large, which makes evaluation of expression (4) very lengthy. Therefore, our aim is to substitute double sum over q and n_q by a single sum over q. To this end we do the following approximation: we substitute the energy E_{q,n_q} in the denominator by the configuration average:

$$\bar{E}_q = \frac{1}{N_q}\sum_{n_q=1}^{N_q} E_{q,n_q}, \tag{5}$$

where N_q is the number of determinants in configuration q. Using this approximation we rewrite (4) in the form

$$\delta E_a = \sum_{p,m_p}\sum_{p',m_{p'}} C^a_{p,m_p}C^a_{p',m_{p'}}\sum_{q} \times \frac{\langle p,m_p|H\left(\sum_{n_q}|q,n_q\rangle\langle q,n_q|\right)H|p',m_{p'}\rangle}{E_a - \bar{E}_q}. \tag{6}$$

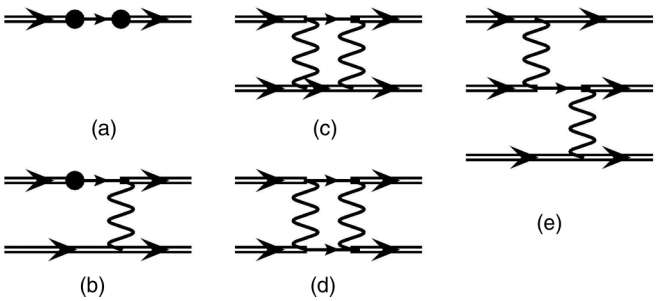

FIG. 1. Set of connected second-order diagrams. Black dots correspond to the core potential and wavy lines to the Coulomb interaction. Double and single lines denote electrons in valence and virtual orbitals respectively. Nonsymmetric diagrams (b) and (e) have mirror twins.

Below we will show that in some very important cases one can get rid of the internal sum over n_q.

Hamiltonian H includes one-particle and two-particle parts. The former consists of the kinetic term and the core potential, while the latter corresponds to the Coulomb (or Coulomb-Breit) interaction between valence electrons. Thus, in the sum over q remain only configurations, which differ by no more than two electrons from configurations p and p'. This means that, within this approximation, the subspace Q is actually truncated to $Q_S + Q_D$. All nonzero contributions correspond to the diagrams, shown in Fig. 1.

According to our definition of the spaces P and Q, the latter must include at least one electron in the virtual shell. Diagrams (a), (b), and (e) include only one intermediate line, so they describe single excitations from the subspace P. Diagrams (c) and (d) include two intermediate lines, but only diagram (d) describes double (D) excitations, because both intermediate lines correspond to the virtual shells.

Figure 1 shows that all many-electron matrix elements in Eq. (6) are reduced to the effective one-electron, two-electron, and three-electron contributions. Effective one-electron contributions are described by diagram (a); diagrams (b), (c), and (d) correspond to the two-electron contributions. Finally, diagram (e) describes effective three-electron contributions.

For combinatorial reasons the number of configurations with two excited electrons is much bigger, than the number of those with only one such electron. Therefore the vast majority of terms in Eq. (6) correspond to the two-electron excitations from configurations p and p'. For these terms in the Hamiltonian H only the two-electron interaction V can contribute, so we can neglect the one-electron part and make substitution $H \to V$. As we saw above, all such terms are described by the single diagram (d) from Fig. 1.

Let us consider the sum over doubly excited configurations. It can be written as

$$\delta E^D_a = \sum_{p,m_p}\sum_{p',m_{p'}} C^a_{p,m_p}C^a_{p',m_{p'}}\sum_{q\in Q_D} \frac{\langle p,m_p|V\left(\sum_{n_q}|q,n_q\rangle\langle q,n_q|\right)V|p',m_{p'}\rangle}{E_a - \bar{E}_q}. \tag{7}$$

Nonzero contributions come from determinants $|q,n_q\rangle$, which differ from both determinants $|p,m_p\rangle$ and $|p',m_{p'}\rangle$ by two electrons. It is clear that it must be the same two electrons, see Fig. 1. In this case, we can explicitly sum over the intermediate magnetic quantum numbers, and thus the second-order expression from (7) is reduced to the effective two-particle

interaction [14]:

$$\delta E_a^D = \sum_{p,m_p} \sum_{p',m_{p'}} C^a_{p,m_p} C^a_{p',m_{p'}} \langle p, m_p | V^{\rm eff} | p', m_{p'} \rangle. \tag{8}$$

The matrix element of this effective interaction $V^{\rm eff}$, which corresponds to the diagram in Fig. 1(d), can be expressed in terms of the multipolar expansion and effective radial integrals $R^{k,\rm eff}_{a,b,c,d}$, similar to the matrix element of the Coulomb interaction:

$$\begin{aligned}\langle c, d | V^{\rm eff}[\text{Fig. 1(d)}] | a, b \rangle = \sum_{k,\varkappa} (-1)^{m_c+m_b+1} \sqrt{(2j_a+1)(2j_b+1)(2j_c+1)(2j_d+1)} \\ \times \begin{pmatrix} j_c & j_a & k \\ -m_c & m_a & \varkappa \end{pmatrix} \begin{pmatrix} j_b & j_d & k \\ -m_b & m_d & \varkappa \end{pmatrix} \begin{pmatrix} j_c & j_a & k \\ \frac{1}{2} & -\frac{1}{2} & 0 \end{pmatrix} \begin{pmatrix} j_b & j_d & k \\ \frac{1}{2} & -\frac{1}{2} & 0 \end{pmatrix} R^{k,\rm eff}_{a,b,c,d},\end{aligned} \tag{9}$$

where round brackets denote $3j$ symbols, j_i and m_i are total angular momenta and their projections on the quantization axis, and k is multipolarity of the effective radial integral. The expression for the latter has the form [14]

$$\begin{aligned} R^{k,\rm eff}_{a,b,c,d} = \sum_{k_1,k_2} \sum_{m,n} (-1)^{\chi} (2j_m+1)(2j_n+1) \\ \times (2k+1) \begin{Bmatrix} j_c & j_a & k \\ k_1 & k_2 & j_m \end{Bmatrix} \begin{Bmatrix} j_b & j_d & k \\ k_2 & k_1 & j_n \end{Bmatrix} \begin{pmatrix} j_m & j_a & k_1 \\ \frac{1}{2} & -\frac{1}{2} & 0 \end{pmatrix} \begin{pmatrix} j_b & j_n & k_1 \\ \frac{1}{2} & -\frac{1}{2} & 0 \end{pmatrix} \\ \times \begin{pmatrix} j_c & j_m & k_2 \\ \frac{1}{2} & -\frac{1}{2} & 0 \end{pmatrix} \begin{pmatrix} j_n & j_d & k_2 \\ \frac{1}{2} & -\frac{1}{2} & 0 \end{pmatrix} \begin{pmatrix} j_c & j_a & k \\ \frac{1}{2} & -\frac{1}{2} & 0 \end{pmatrix}^{-1} \begin{pmatrix} j_b & j_d & k \\ \frac{1}{2} & -\frac{1}{2} & 0 \end{pmatrix}^{-1} \frac{R^{k_1}_{a,b,m,n} R^{k_2}_{c,d,m,n}}{\Delta_E}, \end{aligned} \tag{10}$$

where curly brackets denote $6j$ coefficients, the phase $\chi = j_a + j_b + j_c + j_d + j_m + j_n + k_1 + k_2 + k + 1$, and Δ_E is energy denominator, which we discuss later. Indexes a, b, c, d, and m, n correspond to the orbitals from the subspaces P and Q, respectively.

Let us emphasize that the necessary step, which allows us to express the inner sum in Eq. (4) in terms of the effective radial integrals (10) is the averaging of the energy denominators (5). This is an additional approximation. Some many-electron configurations may include thousands of states and spread over large energy intervals. Thus, it is not obvious that this approximation is sufficiently accurate. Below we made several test calculations for very different systems and showed that error introduced by this approximation is small for all cases considered.

All single excitations are described by the remaining diagrams from Fig. 1. The diagram (a) has a form of the effective one-electron radial integral, while diagrams (b) and (c) are reduced to the two-electron effective radial integrals. In principle, these effective radial integrals can be calculated and stored. However, the diagram (e) corresponds to the effective three-particle interaction. It is difficult to include such interactions into CI matrix for several reasons:

i. When $N > 3$ the number of such effective three-particle integrals is huge.

ii. It is difficult to store them and find them.

iii. The number of the nonzero matrix elements in the matrix drastically increases. The matrix becomes less sparse and its diagonalization is much more difficult and time-consuming.

Because of all that it is inefficient to use the MBPT approach for three-particle diagrams and it is much easier to treat them within the determinant-based PT. However, it is difficult then to separate them from other contributions, which correspond to single excitations. Thus, it is better not to use MBPT for single excitations at all. We suggest to use instead any form of the determinant-based VPT described in Refs. [28–31]. This means that we do VPT in the subspace Q_S. Note that the dimension of this subspace is incomparably smaller than the dimension of the Q_D subspace. In some cases it may be so small that we can include Q_S in the subspace P, where we do CI.

B. Core-valence correlations

It is easy to use the scheme described above for the core-valence correlations as well. Now P subspace corresponds to the frozen-core approximation and the subspaces Q_S and Q_D include single and double excitations from the core, respectively. This means that these subspaces include many-electron states with one and two holes in the core. As before, the second-order MBPT corrections are described by one-electron, two-electron, and three-electron diagrams. All one-electron diagrams are given in Fig. 2. Excitations from the core correspond to the hole lines with arrows looking to the

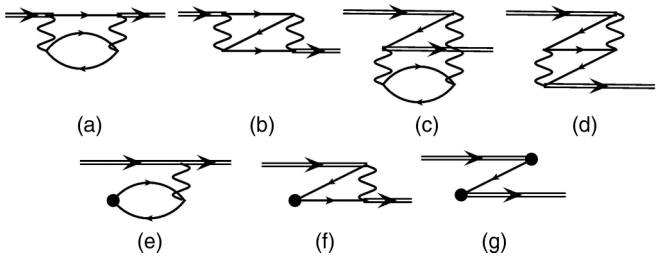

FIG. 2. Set of one-electron second-order diagrams accounting for the excitations from the core. Diagrams (e) and (f) have mirror twins. Diagrams (c) and (d) describe double excitations from the core.

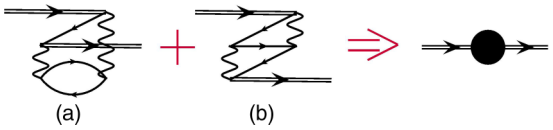

FIG. 3. Diagrams which correspond to the double excitations from closed shells. These diagrams are described by the effective one-electron radial integrals, designated by a black circle.

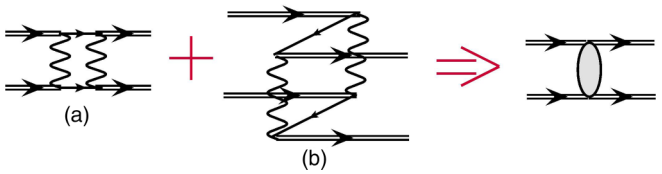

FIG. 4. Diagrams contributing to the effective two-electron radial integrals. The first diagram accounts for the double excitations from the valence to the virtual shells and the second diagram accounts for the double excitations from closed core shells.

left. It is easy to see that only diagrams (c) and (d) describe double excitations. Therefore, we need to calculate them and store as one-electron effective radial integrals, see Fig. 3 (note that there are no one-electron contributions for the valence excitations).

There is only one two-electron diagram, which corresponds to the double excitations from the core. This diagram must be calculated and added to the similar diagram for valence excitations, which was discussed in the previous section, see Fig. 4. Finally, in analogy with the valence correlations, the three-particle diagrams correspond to the single excitations from the core.

We conclude that, to account for both valence and core-valence correlations, we need to calculate one-electron and two-electron effective radial integrals, which correspond to the diagrams from Figs. 3 and 4. At the same time, we need to include all single excitations from the core shells and all single excitations to the virtual shells either in the subspace P or in the subspace Q_S. After that, we make CI calculation with effective radial integrals possibly followed by the VPT calculation in the Q_S subspace.

Expressions (9) and (10) give contributions of the diagram of Fig. 4(a). For the diagram Fig. 4(b) we need to substitute virtual orbitals m, n in Eq. (10) by core orbitals s, t. Expressions for diagrams Figs. 3 were derived in Ref. [14]:

$$\langle b|V^{\rm eff}[\text{Fig. 3(a)}]|a\rangle = -\delta_{j_a,j_b}\delta_{m_a,m_b}\sum_k \frac{(2j_\alpha+1)(2j_s+1)(2j_t+1)}{2k+1} \times \begin{pmatrix} j_a & j_s & k \\ \frac{1}{2} & -\frac{1}{2} & 0 \end{pmatrix}^2 \begin{pmatrix} j_t & j_\alpha & k \\ \frac{1}{2} & -\frac{1}{2} & 0 \end{pmatrix}^2 \frac{R^k_{a,t,s,\alpha}R^k_{b,t,s,\alpha}}{\Delta_E}, \tag{11}$$

$$\langle b|V^{\rm eff}[\text{Fig. 3(b)}]|a\rangle = (-1)^{k_1+k_2+1}\delta_{j_a,j_b}\delta_{m_a,m_b}(2j_\alpha+1)(2j_s+1)(2j_t+1) \times \sum_{k_1,k_2}\begin{Bmatrix} j_a & j_s & k_2 \\ j_\alpha & j_t & k_1 \end{Bmatrix}\begin{pmatrix} j_a & j_s & k_1 \\ \frac{1}{2} & -\frac{1}{2} & 0 \end{pmatrix}\begin{pmatrix} j_t & j_\alpha & k_1 \\ \frac{1}{2} & -\frac{1}{2} & 0 \end{pmatrix}\begin{pmatrix} j_a & j_t & k_2 \\ \frac{1}{2} & -\frac{1}{2} & 0 \end{pmatrix}\begin{pmatrix} j_s & j_\alpha & k_2 \\ \frac{1}{2} & -\frac{1}{2} & 0 \end{pmatrix} \times \frac{R^{k_1}_{a,\alpha,s,t}R^{k_2}_{b,\alpha,t,s}}{\Delta_E}. \tag{12}$$

In the above expressions the indexes a, b and s, t correspond to valence and core orbitals, respectively, while the index α runs over valence and virtual orbitals.

C. Sketch of the possible calculation scheme

Let us describe a most general computational scheme.

i. Basis set orbitals are divided into four groups: inner core, outer core, valence, and virtual orbitals. The inner core is kept frozen on all stages of calculation.

ii. Effective radial integrals are calculated for the valence orbitals, which account for the double excitations from the outer core and the double excitations from the valence orbitals to the virtual ones.

iii. A full CI calculation is done for the valence electrons. The effective radial integrals are added to the conventional radial integrals when the Hamiltonian matrix is formed.

iv. Determinant-based PT is used in the complementary subspace Q_S, which includes single excitations from the outer core and single excitations to the virtual states.

Depending on the number of the valence electrons and the size of the core, this scheme can be simplified. If there are only two valence electrons, one can include all virtual basis states into valence space. Single excitation from the core can be also added to the valence space. Double excitations from the core are accounted for through the effective radial integrals, while single excitations are included explicitly in the CI matrix. Formally this means that we substitute P, Q decomposition by the P', Q_D decomposition:

$$P+Q = P+Q_S+Q_D = P'+Q_D, \tag{13}$$

$$P' \equiv P+Q_S. \tag{14}$$

In the new valence space P', we solve matrix equation with the energy-dependent effective Hamiltonian [14]:

$$H_{\rm eff}(E) = H + V_{\rm eff}(E), \tag{15}$$

$$\hat{P}'H_{\rm eff}(E_a)\hat{P}'\Psi_a = E_a\hat{P}'\Psi_a, \tag{16}$$

where $\hat{P}'$ is the projector on the subspace P'. When the size of the matrix $H_{\rm eff}$ becomes too large, one can neglect the nondiagonal part of the matrix in the Q_S space, as in the emu CI method [29].

III. ENERGY DENOMINATORS

Let us discuss the energy denominator Δ_E in Eq. (10). For simplicity we consider the Rayleigh-Schrödinger perturbation theory, where the denominator in Eq. (6) would be $\bar{E}_p - \bar{E}_q$. Here $\bar{E}_p$ and $\bar{E}_q$ are average energies (5) for configurations p and q. Note that, to return to the Brillouin-Wigner perturbation theory we need to add $E_a - \bar{E}_p$, which can be approximately done using the method suggested in Ref. [14].

In the conventional MBPT the denominator $\bar{E}_p - \bar{E}_q$ is reduced to the difference of the Hartree-Fock energies of the orbitals ε_i which are different in these two configurations. That would give the following energy denominator in Eq. (10):

$$\Delta_E \equiv \Delta_E(ab \to mn) = \varepsilon_a + \varepsilon_b - \varepsilon_m - \varepsilon_n, \tag{17}$$

where we assume that configuration q differs from p by excitation of two electrons from shells a and b to virtual shells m and n, respectively. This expression neglects the interaction of the electrons with each other and depends on the choice of the Hartree-Fock potential. To improve this approximation, we consider general expression for the average energy of the relativistic electronic configuration.

Average energy of the relativistic configuration

The average energy of the relativistic configuration $\bar{E}_p$ [34,35]:

$$\bar{E}_p = \sum_{a\in p} q_a I_a + \tfrac{1}{2}\sum_{a\in p} q_a(q_a-1)U_{aa} + \sum_{a<b;a,b\in p} q_a q_b U_{ab}, \tag{18}$$

where q_a and q_b are occupation numbers for the shells a and b in configuration p and matrix elements of the potential U are given by

$$U_{ab} = \begin{cases} F^0(a,a) + \sum_{k>0} 2f^k_{a,a}F^k(a,a), & a = b \\ F^0(a,b) + \sum_k g^k_{a,b}G^k(a,b), & a \neq b. \end{cases} \tag{19}$$

In these equations I_a is the one-electron radial integral, while $F^k(a,b)$ and $G^k(a,b)$ are standard Coulomb and exchange two-electron radial integrals [35]. The angular factors $f^k_{a,a}$ and $g^k_{a,b}$ are also defined in agreement with Ref. [35]:

$$\begin{aligned} f^k_{a,a} &= -\frac{1}{2}\frac{2j_a+1}{2j_a}\begin{pmatrix} j_a & j_a & k \\ \frac{1}{2} & -\frac{1}{2} & 0 \end{pmatrix}^2, \\ g^k_{a,b} &= -\begin{pmatrix} j_a & j_b & k \\ \frac{1}{2} & -\frac{1}{2} & 0 \end{pmatrix}^2, \end{aligned} \tag{20}$$

where j_a and j_b are the one-electron total angular momenta.

Let us use Eq. (18) to calculate the energy difference between configurations p and q which differ by the excitation of two electrons from shells a, b to shells m, n. In other words we need to calculate how the energy changes when occupation numbers change in the following way: $\delta q_a = \delta q_b = -1$ and $\delta q_m = \delta q_n = 1$. To this end we, can use Taylor expansion of Eq. (18) near the initial configuration p:

$$\bar{E}_q = \bar{E}_p + \sum_a \frac{\partial \bar{E}_p}{\partial q_a}\delta q_a + \frac{1}{2}\sum_{a,b}\frac{\partial^2 \bar{E}_p}{\partial q_a \partial q_b}\delta q_a \delta q_b, \tag{21}$$

where derivatives are given by

$$\begin{aligned} \frac{\partial \bar{E}_p}{\partial q_a} &= I_a + \left(q_a - \frac{1}{2}\right)U_{aa} + \sum_{b\neq a} q_b U_{ab} \\ &= I_a - \tfrac{1}{2}U_{aa} + \sum_b q_b U_{ab}, \end{aligned} \tag{22}$$

$$\frac{\partial^2 \bar{E}_p}{\partial q_a \partial q_b} = U_{ab}. \tag{23}$$

Note that all higher derivatives vanish, so expression (21) is exact. With its help we get

$$\begin{aligned} &\Delta_E(ab \to mn) \\ &= I_a + I_b - I_m - I_n + \sum_{c\in p} q_c(U_{ac} + U_{bc} - U_{mc} - U_{nc}) \\ &\quad - U_{aa} - U_{bb} - U_{ab} - U_{mn} + U_{am} + U_{bn} + U_{an} + U_{bm}. \end{aligned} \tag{24}$$

This expression can be also used for the special cases $a = b$, $\delta q_a = -2$, and/or $m = n$, $\delta q_m = 2$.

Equation (24) includes the sum over the occupied shells of the initial configuration p. Let us introduce one-electron energies in respect to this configuration as

$$\varepsilon_a = I_a + \sum_{c\in p} q_c U_{ac} - (1 - \delta_{q_a,0})U_{aa}. \tag{25}$$

Then Eq. (24) is simplified to

$$\begin{aligned} \Delta_E(ab \to mn) = \varepsilon_a + \varepsilon_b - \varepsilon_m - \varepsilon_n \\ - U_{ab} - U_{mn} + U_{am} + U_{bn} + U_{an} + U_{bm}. \end{aligned} \tag{26}$$

The first line here reproduces the conventional MBPT denominator (17), while the second line gives corrections caused by the interactions of the electrons with each other. It is important that in this form we do not have explicit sums over all electrons, which significantly simplifies calculations.

In the relativistic calculations the nonrelativistic configurations are typically not used. However, sometimes one may need to find the average energy of the nonrelativistic configuration. In the Appendix we derive the necessary expressions for this case.

IV. NUMERICAL TESTS

We made four test calculations for very different systems. In the first two calculations for He I and B I, there was no core and we tested our method for the valence correlations. Then we applied our method for the highly charged ion Fe XVII, where there is a very strong central field, correlation corrections are rather small, and perturbation theory must be quite accurate. In this system we had core $1s^2$, so we calculated core-valence correlation corrections as well as valence ones.

TABLE I. Ground-state binding energy of He I (in a.u.). CI calculations are made for three spaces: P, $P+Q_S$, and $P+Q$. Δ_{P+Q} is the difference from the CI result in the $P+Q$ space. Three variants of PT calculations are made based on the CI calculation in $P+Q_S$ space: (a) determinant-based PT, (b) effective Hamiltonian with Hartree-Fock denominators (17), (c) effective Hamiltonian with corrected denominators (26). Experimental binding energy is given for comparison in the last column [36].

				PT			NIST
	P	$P+Q_S$	$P+Q$	(a)	(b)	(c)	Ref. [36]
$E(1s^2)$	2.8626	2.8700	2.9010	2.9021	2.9064	2.9031	2.9034
Δ_{P+Q}	0.0384	0.0310	0.0000	−0.0011	−0.0054	−0.0021	−0.0024

Finally, we made calculations for Sc I, where valence $3d$ electrons have a large overlap with the core shell $3p^6$ and core-valence correlation corrections are as important as valence ones.

A. Ground state of He I

Helium is the simplest system where correlation effects can be tested. We calculate the ground-state energy, where correlation corrections are the largest. We choose the space P to include shells $n = 1, \ldots, 3$. The space Q includes virtual shells s, p, d with $4 \leqslant n \leqslant 20$. For this model problem, we can easily do CI in the whole space $P+Q$ thus producing the "exact" solution and compare these results with different variants of the perturbation theory discussed above. The results are listed in Table I.

One can see that the valence CI provides accuracy on the order of 1%. The accuracy does not improve when we account for the single excitations to the virtual shells. However, when we include double excitations the agreement with the "exact" answer is significantly better. The determinant-based PT gives the best result. The results obtained with the effective Hamiltonian are less accurate, but corrections to the denominators reduce the discrepancy. Even the uncorrected variant of the MBPT is closer to the "exact" answer by an order of magnitude compared with the valence CI.

B. Ground state of B I

B is a five electron system. The full CI calculation here is already very expensive. The determinant-based PT is also rather lengthy, so we made calculations only with the effective Hamiltonian and compared our results with the experiment [36]. The effective radial integrals were calculated using the Hartree-Fock denominators. We tested two variants of the valence space: the first one, P, included shells $n = 1, \ldots, 3$ and the second one, $\tilde{P}$, included also the shell $n = 4$. Corresponding Q and $\tilde{Q}$ spaces included s, p, d, f, g shells up to $n = 20$. Results of these calculations for the ground state $^2P_{1/2}$ are given in Table II. We see that the accuracy of the CI calculation does not change much when we include an extra shell in the subspace P. The accuracy of the CI calculation in the subspaces $P+Q_S$ and $\tilde{P}+\tilde{Q}_S$ is only slightly better than similar calculation in the subspaces P and $\tilde{P}$. Only including double excitations by means of the MBPT improves the agreement with the experiment by more than an order of magnitude.

C. Spectrum of Fe XVII

Ten-electron ion Fe XVII plays an important role in astrophysics and plasma physics, see Ref. [37] and references therein. The spectrum of this ion was calculated within several different approaches [38] with relative accuracy of about 0.03%. Here we repeat these calculations using the modified method. We use basis set $[17spdfg]$. Virtual orbitals starting from $4s$ and up are formed from B splines using the method from Ref. [39]. Valence subspace P includes shells $2s$, $2p$, $3s$, $3p$, $3d$, $4s$, $4p$, $4d$, and $4f$, while the $1s$ shell is frozen. Single excitations to all higher orbitals are included in the subspace Q_S and the subspace Q'_S in addition includes single excitations from the $1s$ shell. We make two CI calculations in the spaces P and $P+Q_S$, respectively. Then we repeat these calculations using the effective Hamiltonian, which accounts for the excitations to the subspace Q_D. Finally, we make CI calculation in the $P+Q'_S$ for the effective Hamiltonian $H'_{\rm eff}$ which accounts for the double excitations from $1s$ shell as well as for the double excitations to the virtual shells with $n \geqslant 5$. Results of all these calculations are given in Table III.

One can see that already the CI calculation in the subspace P is quite accurate here, the relative errors being about 0.3%. This is not surprising for such a strong central field. When we increase the size of the configuration space by adding single excitations to the virtual shells $n = 5, \ldots, 17$ the errors substantially decrease but remain of the same order of magnitude. The same happens when we do CI for the effective Hamiltonian in the subspace P. Only when we include both single and double excitations to the virtual shells by doing CI for the effective Hamiltonian in the subspace $P+Q_S$ we increase the accuracy by an order of magnitude, the errors being 0.04%

TABLE II. Ground-state binding energy of B I (in a.u.). CI calculations are made for valence spaces P and $\tilde{P}$, which included three and four lower shells, respectively. Experimental binding energy is given for comparison in the last column [36].

		$P+Q_S$			$\tilde{P}+\tilde{Q}_S$		NIST
	P	H	$H_{\rm eff}$	$\tilde{P}$	H	$H_{\rm eff}$	Ref. [36]
$E(^2P_{1/2})$	24.5683	24.5976	24.6595	24.5721	24.5999	24.6581	24.6581
$\Delta_{\rm NIST}$	0.0898	0.0605	−0.0014	0.0860	0.0582	0.0000	0.0000

TABLE III. Low-lying energy levels of Fe XVII in respect to the ground state (in cm^{-1}). The subspace Q_S includes single excitations to virtual shells $n = 5$–17. The subspace Q'_S in addition includes single excitations from the $1s$ shell. Effective Hamiltonians account for the respective double excitations. For each calculation we also give relative accuracy in percent.

		NIST	CI(P)				$CI_{emu}(P+Q_S)$				$CI_{emu}(P+Q'_S)$	
Config.	Level	Ref. [36]	H		H_{eff}		H		H_{eff}		H'_{eff}	
$2p^6$	$^1S_0$	0	0		0		0		0		0	
$2p^5 3p$	$^3S_1$	6093450	6076370	−0.28%	6083540	−0.16%	6088405	−0.08%	6095600	0.04%	6095086	0.03%
$2p^5 3p$	$^3D_2$	6121690	6105049	−0.27%	6111933	−0.16%	6117307	−0.07%	6124215	0.04%	6123709	0.03%
$2p^5 3p$	$^3D_3$	6134730	6118010	−0.27%	6125056	−0.16%	6130067	−0.08%	6137137	0.04%	6136602	0.03%
$2p^5 3p$	$^1P_1$	6143850	6127278	−0.27%	6134193	−0.16%	6139345	−0.07%	6146283	0.04%	6145772	0.03%
$2p^5 3s$	2^o	5849490	5830778	−0.32%	5838679	−0.18%	5842900	−0.11%	5850823	0.02%	5850330	0.01%
$2p^5 3s$	1^o	5864770	5846269	−0.32%	5854109	−0.18%	5858397	−0.11%	5866260	0.03%	5865678	0.02%
$2p^5 3s$	1^o	5960870	5942198	−0.31%	5950103	−0.18%	5954316	−0.11%	5962244	0.02%	5961601	0.01%
$2p^5 3d$	$^3P^o_1$	6471800	6455306	−0.25%	6462010	−0.15%	6463149	−0.13%	6469882	−0.03%	6468962	−0.04%
$2p^5 3d$	$^3P^o_2$	6486400	6470075	−0.25%	6476738	−0.15%	6477839	−0.13%	6484531	−0.03%	6483612	−0.04%
$2p^5 3d$	$^3F^o_4$	6486830	6471630	−0.23%	6478532	−0.13%	6478129	−0.13%	6485057	−0.03%	6484147	−0.04%
$2p^5 3d$	$^3F^o_3$	6493030	6477585	−0.24%	6484338	−0.13%	6484319	−0.13%	6491101	−0.03%	6490177	−0.04%
$2p^5 3d$	$^1D^o_2$	6506700	6491383	−0.24%	6498026	−0.13%	6498360	−0.13%	6505032	−0.03%	6504101	−0.04%

or less. Adding S and D excitations from the $1s$ shell leads to corrections to the transition energies within 0.01%. Our final accuracy is similar to the accuracy obtained in Ref. [38], where CI space included all double and some triple excitations to all virtual shells (the basis set there was different, but of the same length). In our present calculation, the size of the space $P + Q_S$ is about 1.4 million determinants, and the size of the space $P + Q'_S$ is close to 2 million determinants, which is significantly less than the CI space of Ref. [37].

D. Spectrum of Sc I

The ground-state configuration for Sc I is $[Ar]3d^14s^2$ and lowest excited states belong to the configurations $3d^24s$ and $3d4s4p$. The $3d$ shell has a large overlap with the core shells $3s$ and $3p$. Because of that, the frozen-core approximation cannot reproduce even the lowest part of the spectrum. Including $3s$ and $3p$ shells into the valence space makes its size extremely large. Therefore, this is a good system to apply our method.

We use a short basis set $[9spdfgh]$, which is constructed as described in Ref. [39]. In the valence space P, the shells $n \leqslant 3$ are closed and the virtual shells $n \geqslant 8$ and all h orbitals are empty. The space Q_S includes single excitations from the upper core shells $n = 3$ and single excitations to the virtual shells. We keep core shells up to $n \leqslant 2$ frozen on all stages. Results of the calculation of the spectrum are presented in Table IV, where excitation energies from the ground state in cm^{-1} are shown for approximately ten lower levels of each parity. The sizes of the valence space P and $P + Q_S$ are about 6×10^4 and 1×10^6 determinants, respectively. We list the results of three calculations: the full CI in the valence space P and emu CI [29] in the space $P + Q_S$ for the bare and the effective Hamiltonians. The effective radial integrals were calculated with the Hartree-Fock denominators. For each of these calculations we also give differences from the experimental values [36] and the averaged absolute difference.

One can see that all the levels in the CI calculation are shifted from their experimental energies: the levels of the configuration $3d^24s$ lie higher by three thousand inverse centimeters, while the levels of the configuration $3d4s4p$ lie lower by two thousand inverse centimeters. The picture changes drastically when we add single excitations and solve the problem in the space $P + Q_S$. Now the levels of the configuration $3d^24s$ lie lower by three thousand inverse centimeters, while the levels of the configuration $3d4s4p$ are almost in place. Finally, when we use the effective Hamiltonian, which accounts for the double excitations, the levels get closer to their places with the average deviation about 300 cm^{-1}, or seven times smaller, than for the CI calculation.

In this test calculation, we used a rather short basis set and were probably rather far from saturation. Therefore we cannot reliably estimate the ultimate accuracy of the method for scandium. Looking at the results we see that the size of the PT corrections is very large and there is also large cancellation between contributions of the single and double excitations. Therefore, it is unlikely that converged results would be significantly better than what we got here. On the other hand, we see systematic improvement in our final results compared with the pure valence calculation. It is also worth mentioning that, if one would try to include all double excitations in CI calculations, the size of the configuration space would be much above 1×10^8, even for the basis set as short as this one.

V. CONCLUSIONS

We suggest a modified version of the CI + MBPT method [14] with the different division of the many-electron space into parts where nonperturbative and perturbative methods are used. This proposed division may be more practical for the atoms with many valence electrons, where the size of the valence space may be too big for solving the matrix eigenvalue problem. This method can be used in the all-electron calculations for light atoms as well as for the calculations

TABLE IV. Low-lying energy levels of Sc I (in cm^{-1}). For each calculation we also give the differences with NIST [36] and the average absolute difference $|\Delta|_{av} = \frac{1}{k}\sum_{i=1}^{k}|\Delta_i|$. For the CI calculations in the $P + Q_S$ space we use the emu CI approach [29] where we neglect nondiagonal matrix elements in the Q_S subspace. On the diagonal we use averaging over relativistic configurations, see Eq. (18).

		NIST	CI(P)		CI$_{emu}$($P + Q_S$)			
		Ref. [36]	H		H		H_{eff}	
Config.	Level	E	E	Δ	E	Δ	E	Δ
$3d4s^2$	$^2D_{3/2}$	0	0	0	0	0	0	0
	$^2D_{5/2}$	168	147	−21	157	−11	155	−13
$3d^24s$	$^4F_{3/2}$	11520	14945	3425	7361	−4159	11786	266
	$^4F_{5/2}$	11558	14968	3410	7422	−4136	11847	290
	$^4F_{7/2}$	11610	15001	3391	7489	−4121	11914	304
	$^4F_{9/2}$	11677	15047	3370	7541	−4136	11963	285
$3d^24s$	$^2F_{5/2}$	14926	17368	2442	11331	−3595	15661	735
	$^2F_{7/2}$	15042	17455	2413	11453	−3589	15781	739
$3d^24s$	$^2D_{5/2}$	17013	19972	2960	14574	−2439	17475	462
	$^2D_{3/2}$	17025	19980	2955	14601	−2424	17500	475
$3d^24s$	$^4P_{1/2}$	17226	20329	3103	14606	−2620	17472	246
	$^4P_{3/2}$	17255	20339	3084	14679	−2576	17552	297
	$^4P_{5/2}$	17307	20380	3073	14739	−2568	17606	299
$3d4s4p$	$^4F^o_{3/2}$	15673	13921	−1751	16019	346	15872	200
	$^4F^o_{5/2}$	15757	14002	−1754	16099	342	15953	197
	$^4F^o_{7/2}$	15882	14139	−1743	16211	330	16064	183
	$^4F^o_{9/2}$	16027	14290	−1737	16340	314	16194	168
$3d4s4p$	$^4D^o_{1/2}$	16010	14265	−1745	16318	308	16448	438
	$^4D^o_{3/2}$	16022	14311	−1711	16351	329	16517	495
	$^4D^o_{5/2}$	16141	14375	−1766	16403	262	16559	418
	$^4D^o_{7/2}$	16211	14458	−1753	16503	292	16621	410
$3d4s4p$	$^2D^o_{3/2}$	16023	14172	−1851	16516	493	16442	419
	$^2D^o_{5/2}$	16097	14189	−1907	16525	428	16449	352
$3d4s4p$	$^4P^o_{1/2}$	18504	16854	−1650	18528	24	18529	25
	$^4P^o_{3/2}$	18516	16930	−1586	18538	23	18543	27
	$^4P^o_{5/2}$	18571	17007	−1565	18577	6	18572	1
$\|\Delta\|_{av}$			2247		1595		310	

with the frozen core. In the latter case, the single and double excitations from (some of) the core shells can be treated perturbatively. We ran four rather different tests which showed systematic one-order-of-magnitude improvement of the results when we added MBPT corrections to the CI calculations.

ACKNOWLEDGMENTS

We thank Marianna Safronova, Charles Cheung, and Sergey Porsev for their constant interest in this work and very useful discussions. I.I.T. acknowledges the support from the Resource Center "Computer Center of SPbU," St. Petersburg, Russia.

APPENDIX: AVERAGE ENERGY OF THE NONRELATIVISTIC CONFIGURATION

In the average over nonrelativistic configuration (LS average) [40,41], the occupation numbers for the relativistic orbitals q_a may be noninteger, while occupation numbers for nonrelativistic orbitals q_A are still integer (we use capital letters A, B, M, N to designate nonrelativistic orbitals). Below we show that properly defining one-electron integrals I_A and two-electron matrix elements U_{AB} we obtain expressions similar to Eqs. (25) and (26).

The average energy of the nonrelativistic configuration R can be written as

$$\bar{E}_R = \sum_a \tilde{q}_a I_a + \frac{1}{2}\sum_a \tilde{q}_a(\tilde{q}_a - w_a)F^0(a,a) + \sum_{a<b}\tilde{q}_a\tilde{q}_b w_{ab}F^0(a,b) + \sum_{a,k>0}\tilde{q}_a(\tilde{q}_a - w_a)f^k_{aa}F^k(a,a) + \sum_{a<b,k}\tilde{q}_a\tilde{q}_b w_{ab}g^k_{ab}G^k(a,b), \quad \text{(A1)}$$

where

$$\tilde{q}_a = \frac{2j_a+1}{4l_a+2}q_A, \quad w_a = \frac{q_A - \tilde{q}_a + 2j_a}{4l_a+1}, \quad w_{ab} = \begin{cases} \frac{4l_a+2}{4l_a+1}\frac{q_A-1}{q_A}, & A = B \\ 1, & A \neq B. \end{cases} \quad \text{(A2)}$$

Using the expressions

$$\tilde{q}_a(\tilde{q}_a - w_a) = \frac{2j_a+1}{4l_a+2}\frac{2j_a}{4l_a+1}q_A(q_A-1), \quad w_{ab}\tilde{q}_a\tilde{q}_b = \frac{2j_a+1}{4l_a+2}\frac{2j_{a'}+1}{4l_a+1}q_A(q_A-1), \quad A=B, \quad j_a \neq j_{a'}, \tag{A3}$$

we rewrite equation (A1) in the form

$$\begin{aligned}\bar{E}_R = &\sum_A q_A \sum_{j_a}\frac{2j_a+1}{4l_a+2}I_a + \frac{1}{2}\sum_A q_A(q_A-1)\sum_{a,a'\in A}\frac{(2j_a+1)(2j_{a'}+1-\delta_{a,a'})}{(4l_a+2)(4l_a+1)}F^0(a,a')\\ &+\frac{1}{2}\sum_{A\neq B}q_Aq_B\sum_{a\in A,b\in B}\frac{(2j_a+1)(2j_b+1)}{(4l_a+2)(4l_b+2)}\left[F^0(a,b)+\sum_k g^k_{ab}G^k(a,b)\right]\\ &+\frac{1}{2}\sum_A q_A(q_A-1)\sum_{a,a'\in A}\sum_{k>0}\frac{2j_a+1}{4l_a+2}\frac{2j_{a'}+1}{4l_a+1}g^k_{aa'}G^k(a,a').\end{aligned} \tag{A4}$$

In the last sum, the term $k=0$ is absent since $j_a \neq j_{a'}$ and $k \geqslant |j_a - j_{a'}|$. Now we can introduce nonrelativistic analogs of the integrals I_a and matrix elements U_{ab} and rewrite Eq. (A1) like Eq. (18):

$$\bar{E}_R = \sum_A q_A I_A + \frac{1}{2}\sum_A q_A(q_A-1)U_{AA} + \frac{1}{2}\sum_{A\neq B}q_Aq_BU_{AB}, \tag{A5}$$

$$I_A = \sum_{a\in A}\frac{2j_a+1}{4l_a+2}I_a, \tag{A6}$$

$$U_{AA} = \sum_{a,a'\in A}\frac{(2j_a+1)(2j_{a'}+1)}{(4l_a+2)(4l_a+1)}\left[F^0(a,a')+\sum_{k>0}g^k_{aa'}G^k(a,a')\right] - \sum_{a\in A}\frac{(2j_a+1)}{(4l_a+2)(4l_a+1)}F^0(a,a), \tag{A7}$$

$$U_{AB} = \sum_{a\in A,b\in B}\frac{(2j_a+1)(2j_b+1)}{(4l_a+2)(4l_b+2)}\left[F^0(a,b)+\sum_k g^k_{ab}G^k(a,b)\right]. \tag{A8}$$

Using Eq. (A5) we get the following derivatives by analogy with Eqs. (22) and (23):

$$\frac{\partial\bar{E}_R}{\partial q_A} = I_A + \sum_B q_BU_{AB} - \frac{1}{2}U_{AA}, \quad \frac{\partial^2\bar{E}_R}{\partial q_A\partial q_B} = U_{AB}. \tag{A9}$$

The difference in energy between two configurations is

$$\Delta\bar{E} = \sum_A I_A\delta q_A + \sum_A\left(q_A-\frac{1}{2}\right)U_{AA}\delta q_A + \sum_{B\neq A}q_BU_{AB}\delta q_B + \frac{1}{2}\sum_{A,B}U_{AB}\delta q_A\delta q_B. \tag{A10}$$

This equation allows us to find the energy of a double excitation $\delta q_A = -1$, $\delta q_B = -1$, $\delta q_N = 1$, $\delta q_M = 1$:

$$\begin{aligned}\Delta_{\bar{E}}(AB\to NM) = &I_A + I_B - I_M - I_N + \sum_C q_C(U_{AC}+U_{BC}-U_{MC}-U_{NC})\\ &-U_{AA}-U_{BB}-U_{AB}-U_{NM}+U_{AN}+U_{BN}+U_{AM}+U_{BM}.\end{aligned} \tag{A11}$$

If we introduce an averaged one-electron energy by analogy with (25) we can rewrite (A11) as

$$\varepsilon_A = I_A + \sum_B q_BU_{AB} - (1-\delta_{q_A,0})U_{AA}, \tag{A12}$$

$$\Delta_{\bar{E}}(AB\to NM) = \varepsilon_A+\varepsilon_B-\varepsilon_M-\varepsilon_N-U_{AB}-U_{NM}+U_{AN}+U_{BN}+U_{AM}+U_{BM}. \tag{A13}$$

We obtained corrections to the standard MBPT energy denominator (17) using two approximations. Averaging over relativistic configurations gives expression (26) and averaging over nonrelativistic configurations leads to expression (A13). These expressions differ only by the definitions of the one-electron energies and two-electron matrix elements.

[1] J. P. Desclaux, Comput. Phys. Commun. **9**, 31 (1975).

[2] P. Jönsson, G. Gaigalas, J. Bieroń, C. F. Fischer, and I. P. Grant, Comput. Phys. Commun. **184**, 2197 (2013).

[3] C. Froese Fischer, M. Godefroid, T. Brage, P. Jönsson, and G. Gaigalas, J. Phys. B: At., Mol. Opt. Phys. **49**, 182004 (2016).

[4] S. Fritzsche, Comput. Phys. Commun. **240**, 1 (2019).

[5] S. Fritzsche, Atoms **10**, 7 (2022).

[6] S. Fritzsche, C. F. Fischer, and G. Gaigalas, Comput. Phys. Commun. **148**, 103 (2002).

[7] I. I. Tupitsyn, V. M. Shabaev, J. R. Crespo López-Urrutia, I. Draganić, R. S. Orts, and J. Ullrich, Phys. Rev. A **68**, 022511 (2003).

[8] I. I. Tupitsyn, A. V. Volotka, D. A. Glazov, V. M. Shabaev, G. Plunien, J. R. C. López-Urrutia, A. Lapierre, and J. Ullrich, Phys. Rev. A **72**, 062503 (2005).
[9] M. F. Gu, Can. J. Phys. **86**, 675 (2008).
[10] J. Jiang, J. Mitroy, Y. Cheng, and M. W. J. Bromley, Phys. Rev. A **94**, 062514 (2016).
[11] V. A. Dzuba, V. V. Flambaum, P. G. Silvestrov, and O. P. Sushkov, J. Phys. B: At. Mol. Phys. **20**, 1399 (1987).
[12] S. A. Blundell, D. S. Guo, W. R. Johnson, and J. Sapirstein, At. Data Nucl. Data Tables **37**, 103 (1987).
[13] J. Sapirstein, Rev. Mod. Phys. **70**, 55 (1998).
[14] V. A. Dzuba, V. V. Flambaum, and M. G. Kozlov, Phys. Rev. A **54**, 3948 (1996).
[15] M. G. Kozlov, S. G. Porsev, M. S. Safronova, and I. I. Tupitsyn, Comput. Phys. Commun. **195**, 199 (2015).
[16] E. Kahl and J. Berengut, Comput. Phys. Commun. **238**, 232 (2019).
[17] C. Cheung, M. Safronova, and S. Porsev, Symmetry **13**, 621 (2021).
[18] S. A. Blundell, W. R. Johnson, Z. W. Liu, and J. Sapirstein, Phys. Rev. A **40**, 2233 (1989).
[19] M. S. Safronova and W. R. Johnson, Adv. At. Mol. Opt. Phys. **55**, 191 (2008).
[20] E. Eliav and U. Kaldor, *Relativistic Four-Component Multireference Coupled Cluster Methods: Towards A Covariant Approach* (Springer Netherlands, Dordrecht, 2010), pp. 113–144.
[21] T. Saue, R. Bast, A. S. P. Gomes, H. J. A. Jensen, L. Visscher, I. A. Aucar, R. Di Remigio, K. G. Dyall, E. Eliav, E. Fasshauer *et al.*, J. Chem. Phys. **152**, 204104 (2020).
[22] A. V. Oleynichenko, A. Zaitsevskii, L. V. Skripnikov, and E. Eliav, Symmetry **12**, 1101 (2020).
[23] W. R. Johnson, *Atomic Structure Theory. Lectures on Atomic Physics* (Springer, Berlin, Heidelberg, 2007).
[24] V. V. Flambaum and J. S. M. Ginges, Phys. Rev. A **72**, 052115 (2005).
[25] J. S. M. Ginges and J. C. Berengut, Phys. Rev. A **93**, 052509 (2016).
[26] V. M. Shabaev, I. I. Tupitsyn, and V. A. Yerokhin, Phys. Rev. A **88**, 012513 (2013).
[27] I. I. Tupitsyn, M. G. Kozlov, M. S. Safronova, V. M. Shabaev, and V. A. Dzuba, Phys. Rev. Lett. **117**, 253001 (2016).
[28] V. A. Dzuba, J. C. Berengut, C. Harabati, and V. V. Flambaum, Phys. Rev. A **95**, 012503 (2017).
[29] A. J. Geddes, D. A. Czapski, E. V. Kahl, and J. C. Berengut, Phys. Rev. A **98**, 042508 (2018).
[30] V. A. Dzuba, V. V. Flambaum, and M. G. Kozlov, Phys. Rev. A **99**, 032501 (2019).
[31] R. T. Imanbaeva and M. G. Kozlov, Ann. Phys. (Berlin, Ger.) **531**, 1800253 (2019).
[32] C. Cheung, M. S. Safronova, S. G. Porsev, M. G. Kozlov, I. I. Tupitsyn, and A. I. Bondarev, Phys. Rev. Lett. **124**, 163001 (2020).
[33] J. Li and V. Dzuba, J. Quant. Spectrosc. Radiat. Transfer **247**, 106943 (2020).
[34] J. B. Mann, At. Data Nucl. Data Tables **12**, 1 (1973).
[35] I. P. Grant, Adv. Phys. **19**, 747 (1970).
[36] A. Kramida, Y. Ralchenko, J. Reader, and NIST ASD Team, NIST Atomic Spectra Database (version 5.9) (2021); URL https://physics.nist.gov/asd
[37] S. Kuhn, C. Shah, JoseR. Lopez-Urrutia, K. Fujii, R. Steinbrugge, J. Stierhof, M. Togawa, Z. Harman, N. S. Oreshkina, C. Cheung, M. G. Kozlov, S. G. Porsev, M. S. Safronova, J. C. Berengut, M. Rosner, M. Bissinger, R. Ballhausen, N. Hell, S. N. Park, M. Chung, M. Hoesch, J. Seltmann, A. S. Surzhykov, V. A. Yerokhin, J. Wilms, F. S. Porter, T. Stohlker, C. H. Keitel, T. Pfeifer, G. V. Brown, M. A. Leutenegger, and S. Bernitt, Phys. Rev. Lett. **124**, 225001 (2020).
[38] S. Kühn *et al.*, High resolution photoexcitation measurements exacerbate the long-standing fe XVII oscillator strength problem: Supplemental Material (2020); https://journals.aps.org/prl/supplemental/10.1103/PhysRevLett.124.225001/supplement.pdf.
[39] M. Kozlov and I. Tupitsyn, Atoms **7**, 92 (2019).
[40] I. I. Tupitsyn, N. A. Zubova, V. M. Shabaev, G. Plunien, and T. Stöhlker, Phys. Rev. A **98**, 022517 (2018).
[41] I. Lindgren and A. Rosén, in *Case Studies in Atomic Physics*, edited by E. McDaniel and M. McDowell (Elsevier, 1975), pp. 93–196.